



1
2
3
4
5
6
7
8
9
10
11
12
13
14
15
16
17
18
19
20
21
22
23
24
25
26
27
28
29
30
31
32
33
34
35
36
37
38
39
40
41
42
43
44
45
46
47

Improvement of Soil Respiration Parameterization in a Dynamic Global Vegetation Model and Its Impact on the Simulation of Terrestrial Carbon Fluxes

Dongmin Kim¹, Myong-In Lee^{1*}, and Eunkyo Seo¹

¹School of Urban and Environmental Engineering, UNIST, Ulsan, Korea

Corresponding author address: Dr. Myong-In Lee
School of Urban and Environmental Engineering
Ulsan National Institute of Science and Technology,
100 Banyeon-ri, Ulju-gun, Ulsan 689-798, Korea
Email: milee@unist.ac.kr



48 **Abstract**

49 Soil decomposition is one of the critical processes for maintaining a terrestrial ecosystem
50 and the global carbon cycle. The sensitivity of soil respiration (R_s) to temperature, the so-called
51 Q_{10} value, is required for parameterizing the soil decomposition process and is assumed to be
52 a constant in conventional numerical models, while realistically it is not in cases of
53 spatiotemporal heterogeneity. This study develops a new parameterization method for
54 determining Q_{10} by considering the soil respiration dependence on soil temperature and
55 moisture obtained by multiple regression. This study further investigates the impacts of the
56 new parameterization on the global terrestrial carbon flux. Our results show that non-uniform
57 spatial distribution of Q_{10} tends to represent the dependence of the soil respiration process on
58 heterogeneous surface vegetation type compared with the control simulation using a uniform
59 Q_{10} . Moreover, it tends to improve the simulation of the observed relationship between soil
60 respiration and soil temperature and moisture, particularly over cold and dry regions. The new
61 parameterization improves the simulation of gross primary production (GPP). It leads to a more
62 realistic spatial distribution of GPP, particularly over high latitudes (60–80 N) where the
63 original model has a significant underestimation bias. In addition, overestimation bias of GPP
64 in the tropics and the midlatitudes is significantly reduced. Improvement in the spatial
65 distribution of GPP leads to a substantial reduction of global mean bias of GPP from + 9.11 to
66 + 1.68 GtC yr⁻¹ compared with the FLUXNET-MTE observation data.

67

68



69 **1. Introduction**

70 Vegetated land surface affects climate (Foley et al., 1998; Sellers et al., 1986) and is affected
71 by climate significantly (Bonan, 2008), forming complex interactions and feedback loops
72 critical to climate change (Friedlingstein et al., 2006; Gregory et al., 2009). The land surface
73 components of Earth System Models (ESMs) have evolved from only representing biophysical
74 processes (i.e., hydrology and energy cycling) to including biogeochemical processes, such as
75 dynamic vegetation change and carbon and nutrient cycles driven by ecosystems (Oleson et al.,
76 2013; Sitch et al., 2003; Wang et al., 2010). The carbon balance of terrestrial ecosystems is the
77 result of the balance between carbon uptake and loss by plants and soil respiration (Beer et al.,
78 2010; Malhi et al., 1999; Le Que re et al., 2009, 2014; Luysaert et al., 2007; Trumbore, 2006).
79 Which terrestrial ecosystems act dominantly as sinks or sources has been a subject of
80 considerable interest in studies of future climate change. Precise evaluation for each sink and
81 source component and their responses to environmental factors are essential for reliable
82 projection of future climate change by ESMs.

83 Future climate change projection by various ESMs is diverse and highly uncertain
84 (Friedlingstein et al., 2006). One of the main causes seems to be related to our poor knowledge
85 on carbon exchange by soil, leading to significant diversity among the model simulations.
86 Diversity in the parameterization of photosynthesis at the leaf level is small compared with that
87 of the soil decomposition process in contemporary ESMs with an interactive carbon cycle.
88 Microbial decomposition of soil organic matter produces a major carbon flux from the
89 subsurface biosphere. A few studies suggest that global warming would be accelerated by the
90 release of CO₂ from soil (e.g., Suseela et al., 2012). However, the amplitude of the soil
91 decomposition process has not been quantified and is highly uncertain, mostly due to the lack
92 of observation data and poor estimates of it based on soil temperature (Sussela et al., 2012).
93 The reduction of uncertainty in the soil biogeochemical process remains a challenge for the



94 ESM modeling community.

95 Soil respiration (R_s) is considered a significant source of CO_2 from terrestrial ecosystems.

96 Recent studies suggest that CO_2 emission change by soil should be largely driven by surface
97 temperature change (Bond-Lamberty and Thomson, 2010). At global, regional and local scales,
98 soil temperature and soil moisture are considered the most important abiotic parameters
99 determining R_s (Kutsch et al., 2009). Empirical response functions based on heterogeneous
100 field measurements are commonly used to derive annual estimates of R_s (Tang et al., 2005).

101 The sensitivity of soil respiration (R_s) to temperature, the so-called Q_{10} value, is required
102 for parameterizing the soil decomposition process. Despite a lack of observation data from field
103 studies for R_s and its dependence on soil temperature, some previous studies have suggested
104 that the Q_{10} value derived from soil respiration measurement tends to decrease with
105 temperature because substrate availability decreases as temperature increases (Belay-Tedla et
106 al., 2009). All the abiotic and biotic factors such as soil temperature (Lloyd and Taylor, 1994;
107 Kirschbaum, 1995; Luo et al., 2001), moisture (Davidson et al., 1998; Reichstein et al., 2002;
108 Hui and Luo, 2004), and soil organic matter (Taylor et al., 1989; Liski et al., 1999; Wan and
109 Luo, 2003) are heterogeneous, showing substantial spatial variation globally. Accordingly,
110 estimated Q_{10} from measured soil respiration possibly varies at various geographic locations
111 (Xu and Qi, 2001).

112 Based on the aforementioned studies, Zhao et al. (2009) developed an inverse model to
113 retrieve the global pattern of heterogeneous Q_{10} values by assimilating soil organic carbon
114 data with a process-based biogeochemical model. They suggested that spatial distribution of
115 Q_{10} values changes according to vegetation type, with an increasing tendency as latitude
116 increases. The impact on the estimation of carbon release due to Q_{10} variation in space is a
117 significant change of approximately 25–40 % compared with the use of a constant Q_{10} value
118 in Zhao et al. (2009). This result suggests that the determination of Q_{10} value is very important



119 for the simulation of carbon-climate feedback and future climate change. However, most
120 advanced ESMs that participated in Coupled Model Intercomparison Project Phase 5 (CMIP5)
121 still use a globally constant Q_{10} value in the dynamic global vegetation model. In this case, the
122 sensitivity of subsurface carbon flux under global warming condition would not be reflected in
123 the model simulation.

124 Motivated by the above, this study developed a new parameterization method for
125 determining Q_{10} by considering the dependence of soil respiration on soil temperature and
126 moisture, the relationship of which was obtained from multiple regression with those two
127 predictors. The variation of dominant vegetation type for the given area was also considered
128 when determining Q_{10} . Community Land Model version 4 (CLM4) has the parameterization
129 of the interactive carbon and nitrogen (C-N) cycle for the dynamic vegetation model, which
130 was used to derive realistic spatial distributions of Q_{10} . This study further investigates the
131 impacts of the new parameterization on the global carbon cycle.

132 Section 2 describes the observation and modeling data used in this study and the modeling
133 method used to obtain the distribution of Q_{10} . Section 3 provides the results from the off-line
134 dynamic vegetation model test with prescribed atmospheric states. In addition, the results from
135 a fully interactive ESM model test with the modified Q_{10} are provided in that section.
136 Summary and further discussion are provided in Section 4.

137

138 **2. Data, Methods, and Experiments**

139 **2.1. Data**

140 FLUXNET-MTE (Multi Tree Ensemble) data (Jung et al., 2009) is used to validate GPP.
141 FLUXNET provides the global distribution of carbon and water fluxes in the vegetated land
142 surface and its temporal variation, which were derived from upscaling eddy covariance
143 measurements at the flux tower sites using a statistical machine-learning algorithm. The data



144 provide the information on terrestrial carbon and water cycles globally (Jung et al. 2009). The
145 data's spatial resolution is $0.5^\circ \times 0.5^\circ$ (lat./lon.) and is monthly for 23 years (1983–2009).

146 This study also used the Moderate Resolution Imaging Spectroradiometer (MODIS) GPP and
147 net primary production (NPP) data. Autotrophic respiration (R_a) by plants was determined by
148 subtracting NPP from GPP by definition. This study used the gridded data for the global
149 domain at $0.5^\circ \times 0.5^\circ$ horizontal resolution. These data are originally from MODIS17A3 GPP
150 and NPP products in HDF EOS (Hierarchical Data Format – Earth Observing System) format
151 with a native resolution of 1 km (Running et al., 2004). Each tile is 1200 X 1200 km (Zhao et
152 al., 2005).

153 When GPP is compared between in situ observation-based FLUXNET-MTE and satellite-
154 based MODIS, the two datasets show a minor difference for the overlapping period (2000–
155 2006). The global GPP of FLUXNET-MTE is $101.13 \text{ GtC yr}^{-1}$ and that of MODIS is 100.51
156 GtC yr^{-1} , which is less than 1 % of the total value.

157 Soil respiration (R_s) was verified using the data from Hashimoto et al. (2015). The data were
158 also used for the parameterization of soil respiration (described in detail in Section 2.2).
159 Although only directly observed soil respiration is available from SRDB data version 3 (Bond-
160 Lamberty and Thomson, 2010), it has limited sampling for boreal cold regions (i.e., tundra and
161 northern Siberian) as well as unpopulated regions in the tropics, covering a significant portion
162 of the global biosphere. The data from Hashimoto et al. were derived using SRDB data and the
163 empirical soil respiration model with specified climate conditions for surface air temperature
164 and precipitation. The model was modified and updated from the original version of Raich et
165 al. (2002). Global land use data in a synergetic land cover product (SYNMAP, Jung et al., 2006)
166 using a Bayesian calibration scheme were used to determine the best parameter set for
167 assuming the climate-driven model of soil respiration. The climate-forcing data were obtained
168 from CRU version 3.21 climate data (University of East Anglia Climatic Research Unit, 2013).



169 These data was applied monthly at a spatial resolution of $0.5^\circ \times 0.5^\circ$ (lat./lon.).

170 All the data were regridded onto $1.9^\circ \times 2.5^\circ$ lat./lon. grids for comparison with the CLM4

171 simulation at this resolution.

172

173 2.2. Q10 Parameterization

174 Most dynamic vegetation models implemented in current ESMs, including CLM4, adopt a

175 simple type of empirical equation for R_s , which is proportional to the soil decomposition flux

176 of carbon at the root zone. The decomposition flux is calculated by multiplying the carbon

177 amount from dead leaf by the rate scalar (R_{scalar}), representing the effects of the physical

178 environmental condition such as soil temperature (T_{scalar}) and moisture (W_{scalar}) as:

$$179 \quad R_{scalar} = T_{scalar} * W_{scalar}, \quad (1)$$

180 where T_{scalar} is basically an exponential function of temperature from van't Hoff (1898). It is

181 implemented in CLM4 as in the following equation:

$$182 \quad T_{scalar} = Q_{10}^{\left[\frac{T_j - T_{ref}}{10}\right]}, \quad (2)$$

183 where T_j is the temperature at the j -th soil level, and T_{ref} is the reference temperature of 25

184 °C. CLM4 considers temperature for the top 5 soil levels as representing the root zone (approx.

185 29 cm depth). Q_{10} is specified as a constant value of 1.5 in the standard CLM4 model. The

186 moisture scalar (W_{scalar}) is based on Andren and Paustian (1987), which describes the potential

187 for soil water decomposition as

$$188 \quad W_{scalar} = \sum_{j=1}^5 \frac{\log\left(\frac{\psi_{min}}{\psi_j}\right)}{\log\left(\frac{\psi_{min}}{\psi_{max}}\right)}, \quad (3)$$

189 where ψ_j is the soil water potential at the level j defined from the exponential of volumetric



190 soil moisture ($\text{m}^3 \text{m}^{-3}$). Ψ_{max} is the maximum potential depending on soil type, and Ψ_{min} is
 191 the minimum value of -10 MPa, regardless of soil type. The range of W_{scalar} is 0 to 1 by
 192 setting to 0 when the Ψ_j is below Ψ_{min} , and setting to 1 when Ψ_j is above Ψ_{max} .

193 For improving the R_s parameterization in CLM4, this study considers a spatiotemporal
 194 change of Q_{10} in (2). We developed a multiple regression model for Q_{10} based on Qi et al.
 195 [2002], which assumes that the rate of R_s change depends entirely on soil temperature (T) and
 196 soil moisture (M). These two physical variables are well-known important factors for soil
 197 biological processes. The fractional instantaneous change of R_s by soil temperature q is defined
 198 as

$$199 \quad q(T, M) = \frac{1}{R_s} \frac{dR_s}{dT} \quad (4)$$

200 Q_{10} is defined as the relative change of R_s at a temperature increase of 10 degrees, which
 201 can be described in the following equations:

$$202 \quad Q_{10}(T, M) = \frac{R_s(T + 5, X)}{R_s(T - 5, X)} \quad , \quad (5)$$

$$203 \quad Q_{10} = e^{\int_{T-5}^{T+5} q(T, X) dT} \quad , \quad (6)$$

204 where X is any additional independent variable to predict R_s . In this case, only soil moisture
 205 (M) is considered. From (6), Q_{10} is a monotonic function of q , and the factor affecting q also
 206 influences Q_{10} . Therefore, the change of R_s is decomposed into the change by temperature
 207 and the change by moisture:

$$208 \quad \frac{dR_s}{dT} = \frac{\partial R_s(T, M)}{\partial M} \frac{dM}{dT} + \frac{\partial R_s(T, M)}{\partial T} \quad . \quad (7)$$

209 Inserting (7) into (4), the equation for q is rewritten as

$$210 \quad q(T, M) = \frac{1}{R_s} \left[\frac{\partial R_s(T, M)}{\partial M} \frac{dM}{dT} + \frac{\partial R_s(T, M)}{\partial T} \right] \quad , \quad (8)$$



211 where $dM/dT = -1/2.2 = -0.455$, as suggested by Xu and Qi (2001).

212 Through a multiple regression analysis, the relationships between R_s and T and between
213 R_s and M were obtained. In this study, multiple regression was conducted for each plant
214 function type (PFT) for 16 classifications in CLM4. The Q_{10} multiple regression model
215 developed in this study has an advantage over the treatment of constant value in the standard
216 CLM4 model. First, the dependence of R_s on soil moisture and temperature can be dependent
217 on PFT. In addition, this approach is able to consider the nonlinear relationship between R_s
218 and the two major environmental variables of soil temperature and moisture, supported by
219 recent observational studies (Davidson et al., 1998; Raich et al., 2002).

220 Crucial for the parameterization of Q_{10} are the quality of the reference data and the degree
221 of fitting for multiple regression. The observation data for R_s were obtained from Hashimoto
222 et al. (2015) soil respiration data. The parametrization requires the dependence of soil
223 respiration on subsurface temperature and moisture; these data are also not available from in
224 situ observations. To obtain these variables, this study conducted a land surface reanalysis for
225 the most recent 30 years (1981–2010), using the off-line land-surface model driven by observed
226 meteorological forcing data from Sheffield et al. (2006). The forcing data by Sheffield et al.
227 consist of the observation-based datasets of precipitation, air temperature, and radiation. The
228 Global Precipitation Climatology Project (GPCP; Huffman et al., 2001) and the Tropical
229 Rainfall Measuring Mission (TRMM; Huffman et al. 2003) 3B42RT were utilized for the
230 rescaling of daily and 3-hour precipitation, respectively. The surface temperature observation
231 is based on the Climatic Research Unit (CRU) 2.0 product (Mitchell et al. 2004). The radiation
232 data was based on the NASA Langley monthly surface radiation budget (Stackhouse et al.,
233 2004). Remaining meteorological conditions, such as surface wind and humidity, were from
234 the National Centers for Environmental Prediction–National Center for Atmospheric Research
235 (NCEP-NCAR) atmospheric reanalysis. The offline land-surface model integration was



236 conducted with 3-hour forcing data. Our detailed procedure of the off-line land-surface model
237 integration is also found in Seo et al. (2016, in manuscript).

238 Figure 1 shows the r-squared values from the multiple regression for soil respiration for
239 various PFT types. In most vegetation types, the regression by soil temperature and moisture
240 tends to exhibit high values close to 1. The regression results are better than they are when the
241 multi-model ensemble average of soil temperature and moisture from 13 Global Soil Wetness
242 Project (GSWP2) land surface model outputs (Dirmeyer et al., 2006) were applied to the
243 multiple regression. This difference is attributed mostly to a better quality of forcing data by
244 Sheffield et al. (2006), such as the use of daily precipitation data instead of monthly values in
245 GSWP2 and a longer training period from 1983–2010 than was used for GSWP2 data (1986–
246 1995). The r-square value was found to be comparable when the period of forcing data was
247 reduced.

248

249 **2.3. Experiments**

250 Two sets of off-line CLM4 simulations were conducted with identical meteorological forcing
251 for 23 years (1983–2005), where the only difference was the specification of Q10 in the control
252 run (CTL) and the state-dependent Q10 in every time interval (EXP). Figure 2 shows the time
253 average of Q10 values, where the geographical change is clear according to the dominant PFTs
254 and climate conditions. Generally, the regions of lower canopy plants with cold soil
255 temperatures exhibit relatively higher values, significantly higher than the default value of 1.5
256 in CTL. In contrast, the regions of lower Q10 values are located at low latitudes in high
257 temperatures, such as the Amazon and the Maritime Continent. This result suggests that soil
258 respiration is more sensitive to the change of soil temperature in boreal vegetated regions in
259 cold climates.

260 The time average of the off-line simulation from the standard run (CTL) in Figure 3 is very



261 similar to the fully interactive integration of the same model in terms of the spatial bias pattern
262 for the terrestrial carbon fluxes, presumably inherited by the deficiencies in the parametrization
263 of the dynamic vegetation model. Both simulations tend to overestimate GPP over the tropics
264 and underestimate it in high latitudes. The bias pattern of R_s is also quite similar with no
265 significant difference. Despite the fact that in the simulated climatic condition the fully
266 interactive run should be different from the observation used to drive the off-line CLM4, much
267 resemblance in the terrestrial carbon-flux bias pattern suggests that the deficiency in the
268 dynamic vegetation model is overwhelming the bias rather than that systematic error is
269 occurring in the climate condition. Therefore, our comparison in the following sections is
270 mostly for the off-line simulation differences between CTL and EXP.

271

272 3. Results

273 3.1. GPP simulations by CMIP5 ESMs

274 Figure 4 compares the zonal mean distribution of GPP averaged for 23 years (1983–2005)
275 between FLUXNET-MTE observations and the historical emission-driven simulations by
276 CMIP5 ESMs. Among the models, the two ESMs from CESM-BGC and NorESM share an
277 identical dynamic vegetation model with an interactive C-N cycle (Bonan et al., 2011). The
278 global GPP simulated by the multi-model ensemble (MME) of CMIP5 ESMs is $119.28 \text{ GtC yr}^{-1}$
279 ¹, which is a slight overestimation by 18 GtC yr^{-1} from the FLUXNET-MTE observation.
280 Overall, MME shows realistic meridional variation with large values in the tropics and small
281 values in high latitudes. As identified in previous studies, however, the ESMs tend to
282 overestimate GPP significantly in the tropics (Shao et al., 2013; Anav et al., 2013). Global GPP
283 simulated by the two ESMs with an interactive C-N cycle is lower than the remainder of the
284 ESMs (-12 GtC yr^{-1}). Including typical biases of overestimation of GPP over tropical belts
285 (20S–20N), the two models show the other GPP bias from the remainder of the ESMs, which



286 tend to significantly underestimate GPP, even more so than other ESMs in the Northern
287 Hemisphere high latitudes (> 60 N). These systematic biases are a common problem in the C-
288 N coupled models based on CLM4 (Bonan et al., 2011; Thornton et al., 2009). These two are
289 major GPP regions, where the model biases are crucial to the uncertainty of the future climate
290 change projections.

291

292 **3.2. Sensitivity to the Q10 parametrization**

293 Figure 5 shows the spatial distribution of GPP from the observations and the offline
294 control CLM4 simulation with the standard model (CTL). Although the simulated pattern of
295 GPP is generally consistent with the FLUXNET observation, the model also exhibits the
296 systematic biases clearly, such as significant overestimation of GPP in the tropical belts. Figure
297 5 also compares the R_s pattern between the observation and the offline model simulation. The
298 simulated pattern also shows a general agreement with the observation, such as large soil
299 respiration in warm and wet regions in low latitudes and less respiration in cold and dry regions
300 in high latitudes. However, the simulation bias in CTL shows the uniform pattern of
301 underestimation in almost every region except central China. This bias suggests that the
302 parameterization of internal soil biological processes could be misrepresented in the standard
303 CLM4 model.

304 The R_s simulation difference between CTL and EXP is given in Figure 5, in terms of
305 global distribution as well as zonally-averaged distribution. Overall, the modification to Q10
306 tends to increase R_s in almost every region. This is an improvement from CTL, although the
307 model now tends to overestimate R_s in some specific regions, such as the tropics and the high
308 latitudes in the Northern Hemisphere, such as southern Siberia, Alaska and China. Overall the
309 increase of R_s can be attributed to the increase of Q10 in most of the vegetated regions (Figure
310 2) from the standard value of 1.5. Despite the increase of R_s in EXP, the underestimation



311 persists over the Amazon and other large biomass regions.

312 The Q10 parametrization tends to enhance the relationship between R_s and soil
313 temperature from CTL (Figure 6). First, simulated R_s by EXP is larger than that of CTL in most
314 PFTs, and the difference between EXP and CTL increases with temperature. This sensitivity
315 also depends on the surface vegetation type. The temperature sensitivity is particularly strong
316 in boreal and tropical plant types. This relationship is rather unclear in the temperate plant type,
317 which seems to suggest the role of soil moisture in this vegetation type. The samples for the
318 grass type are too small to detect the sensitivity. The different sensitivities should be linked to
319 changes in Q10 values in EXP from CTL (Table 1). The Q10 value has been increased for the
320 boreal forest and boreal shrubs in EXP; whereas, it has been decreased or has no significant
321 change in the temperate forest type. This result is consistent with the parameterization for Q10
322 in Equation (2).

323 Figure 7 compares the GPP bias patterns in CTL and EXP. CTL shows significant biases
324 when sign and magnitude differ geographically. Among the biases, overestimation in the
325 tropics and underestimation in Siberia is evident. Although the spatial structure of bias seems
326 to be quite similar, implying intrinsic model deficiencies other than Q10, EXP shows an
327 improvement by reducing biases such as overestimation in southern Asia and China and
328 underestimation in northern Eurasia in CTL. However, underestimation biases in the central
329 part of North America and the Amazon are even larger in EXP. This change of spatial
330 distribution of GPP is associated with sensitivity of R_s and soil temperature. Degradation of
331 GPP simulation over Europe and North America is driven by the temperate plant type where
332 the temperature sensitivity of R_s tends to decrease (Figure 6). On the other hand, the northern
333 Eurasian and Chinese regions that have good improvement of GPP bias in EXP show an
334 enhanced relationship between R_s and temperature. This result indicates that the change of R_s
335 to soil temperature by Q10 variation affects not only the change in respiration but also the



336 carbon production (GPP) flux.

337 The improvement in the GPP simulation by the Q10 parameterization is illustrated better
338 in Figure 8, which compares the regionally averaged GPP over major 4 regions. In the global
339 average, EXP reduces the overestimation bias by approximately 10 % (103.81 GtC/yr)
340 compared with CTL simulation (111.24 GtC/yr). Little plant cover over SH (60S-20S) leads
341 to a smaller contribution of global GPP. The improvement over this region is not clear in EXP.
342 However, the overestimation bias in the tropical regions has been improved significantly. This
343 result is caused by the suppression of the GPP amount in the Amazon region in EXP. This
344 underestimation of GPP over the Amazon induces the improvement of the zonal mean
345 terrestrial carbon budget in EXP. The middle latitude region (20N–60N), which is dominated
346 by temperate forest and crop fields, also has a reduced overestimation of GPP bias compared
347 with CTL. In addition, simulated GPP over high latitude regions (> 60N) were improved in
348 EXP. Those were also the common areas of bias in the interactive C-N coupled ESM run.

349 The modification to the soil process parameterization can affect the rest of the terrestrial
350 carbon cycle by changing the carbon pool in the soil system for plant assimilation. For detailed
351 investigation of the impact of the Q10 parameterization, this study further investigates the
352 changes in the simulated terrestrial carbon cycle of each vegetation type. Figure 9 compares
353 the observation and the simulations using two offline runs for GPP, autotrophic respiration by
354 plants (R_a), and R_s depending on the primary vegetation type. For the comparisons of GPP and
355 R_a , satellite-based MODIS data were used as the data separated GPP and R_a over vegetation
356 areas. In the MODIS observations, the terrestrial carbon cycle is largely contributed to by
357 vegetation response in tropical and temperate tree regions. Vegetation types with a short canopy
358 height and trees with deciduous leaves contribute less in terms of absolute amount of carbon
359 fluxes, although their relative changes are not trivial. Both CTL and EXP runs capture these
360 observed differences in the magnitude of carbon fluxes realistically. Regarding the simulation



361 of GPP, EXP tends to reduce the biases, particularly in temperate, tropical and crop zones. EXP
362 also improves the simulation of R_a in those regions. The improvement is most evident in R_s ,
363 where the simulated values are close to the observed values in most vegetation types. R_s by
364 EXP has been increased in every type of vegetation from CTL, reaching values closer to the
365 reference observation data. According to this result, although the absolute magnitude of R_s is
366 much smaller compared with that of GPP and R_a , the modification of R_s by the Q10
367 parameterization affects the entire terrestrial carbon cycle and improves their simulations.

368

369 **4. Summary and Concluding Remarks**

370 Soil respiration is a crucial process in maintaining terrestrial carbon cycles. Although its
371 sensitivity to the physical environmental conditions such as soil temperature and moisture
372 depends on the type of vegetation, as supported by observational data, most contemporary
373 ESMs do not consider this dependence. These models thereby underestimate the effects of and
374 feedbacks from soil respiration on terrestrial carbon cycles. Using the CLM4 land surface
375 model with the interactive C-N cycle, this study developed a new parameterization method to
376 consider the spatiotemporal variation of Q10 that represents the sensitivity of soil respiration
377 to the temperature change for each different vegetation type. This sensitivity has been treated
378 as constant with a uniform value regardless of plant type in the original CLM4 model.

379 The new parameterization changes the simulation of soil respiration and the rest of
380 terrestrial carbon fluxes significantly by enhancing the feedback to the plant production process.
381 The new parameterization calculates Q10 at every time interval for each location, and this state-
382 dependent prescription induces the overall increase of soil respiration in most locations and
383 most vegetation types, improving spatially uniform negative bias in the original CLM4
384 simulation with constant Q10 value. The simulated sensitivity of soil respiration to soil
385 temperature and moisture by the new method showed more realistic features, particularly in



386 the temperate and cold regions. This changed soil carbon fluxes at the subsurface and affected
387 the simulation of GPP, where the simulation of spatial distribution of GPP has been improved
388 particularly over high latitudes with short canopy heights and over the tropics and warm regions,
389 including southern Asia and China. The improved GPP simulation over cold regions was
390 mostly attributed to the increase in carbon decomposition in those regions. Due to the
391 advancement of both respiration and primary production, carbon balance between subsurface
392 and surface ecosystems with soil organic matter and plants were also improved by the new Q10
393 parameterization. The observed ratio of soil respiration to GPP was represented better in the
394 new simulation, which clearly shows the dependence on the vegetation type.

395 The major findings from this study suggest that the modification of subsurface terrestrial
396 carbon cycle processes is important for improving the simulation of terrestrial carbon fluxes.
397 The parameterization of the photosynthetic process is still a major term crucially related to
398 primary production (Bonan et al. 2010; Bonan et al., 2011). Previous studies have suggested
399 that the improvement of canopy processes in the photosynthetic parameter in CLM4 was able
400 to improve the simulation by reducing the overestimation of GPP in the tropics. Despite the
401 improvement in the photosynthetic process in their models, respiration processes by plants and
402 soil are still largely uncertain due to a lack of reliable observational data and comprehensive
403 studies. For this reason, this study approached the modification of the soil decomposition
404 process, aiming to improve the terrestrial carbon cycle. In fact, the parameterization of
405 photosynthesis is more or less similar, with small differences in current ESMs. Still, large
406 uncertainties lie in the formulation of the respiration process and its parameters. This study
407 suggested that the improved soil decomposition process induces a change in carbon-climate
408 feedback intensity by changing soil respiration. In addition, the realistic description of Q10
409 variation in a numerical model will reduce the uncertainty of the magnitude of carbon-climate
410 feedback due to accurate atmospheric CO₂ simulation in ESMs.



411

412

413 **Acknowledgement**

414 This study is supported Basic Science Research Program through the National Research
415 Foundation of Korea (NRF), funded by the Ministry of Education, Science and Technology
416 (2012M1A2A2671851) and the Supercomputing Center/Korea Institute of Science and
417 Technology Information with supercomputing resources including technical support (KSC-
418 2015-C3-035).

419

420

421

422



423 **References**

- 424 Anav, A., Friedlingstein, P., Kidston, M., Bopp, L., Ciais, P., Cox, P., Jones, C., Jung, M.,
425 Myneni, R., and Zhu, Z.: Evaluating the land and ocean components of the global carbon cycle
426 in the CMIP5 Earth System Models, *J. Clim.*, 26, 6801–6843, doi:10.1175/JCLI-D-12-00417.1,
427 2013.
- 428 Andren, O., Paustian, K.: Barley Straw Decomposition in the Field: A Comparison of Models,
429 *Biology*, 68, 1190-1200, doi:10.2307/1939203, 1987.
- 430 Arora, V. K., Boer, G. J., Friedlingstein, P., Eby, M., Jones, C. D., Christian, J. R., Bonan,
431 G., Bopp, L., Brovkin, V., Cadule, P., Hajima, T., Ilyina, T., Lindsay, K., Tjiputra, J. F., Wu, T.:
432 Carbon–concentration and carbon–climate feedbacks in CMIP5 earth system models, *J. Clim.*,
433 26, 5289-5314, doi:10.1175/JCLI-D-12-00494.1, 2013.
- 434 Beer, C., Reichstein, M., Tomelleri, E., Ciais, P., Jung, M., Carvalhais, N., Rodenbeck, C.,
435 Arain, M. A., Baldocchi, D., Bonan, G. B., Bondeau, A., Cescatti, A., Lasslop, G., Lindroth,
436 A., Lomas, M., Luysaert, S., Margolis, H., Oleson, K. W., Rouspard, O., Veenendaal, E., Viovy,
437 N., Williams, C., Woodward, F. I., and Papale, D.: Terrestrial Gross Carbon Dioxide Uptake:
438 Global Distribution and Covariation with Climate, *Science*, 329, 834-838, 2010.
- 439 Belay-Tedla, A., Zhou, X. H., Su, B., Wan, S. Q., and Luo, Y. Q.: Labile, recalcitrant, and
440 microbial carbon and nitrogen pools of a tallgrass prairie soil in the US Great Plains subjected
441 to experimental warming and clipping, *Soil Biol. Biochem.*, 41, 110–116, 2009.
- 442 Bonan, G. B.: Forests and Climate Change: Forcings, Feedbacks, and the Climate Benefits
443 of Forests, *Science*, 320, 1444-1449, 2008.
- 444 Bonan, G. B., Lawrence, P. J., Oleson, K. W., Levis, S., Jung, M., Reichstein, M., Lawrence,
445 D. M., and Swenson, S. C.: Improving canopy processes in the Community Land Model
446 version 4 (CLM4) using global flux fields empirically inferred from FLUXNET data, *J.*
447 *Geophys. Res.*, 116, G02014, doi:10.1029/2010JG001593, 2011.



448 Bonan, G. B., and Levis S.: Quantifying carbon-nitrogen feedbacks in the Community Land
449 Model (CLM4), *Geop.hys. Res. Lett.*, 37, L07401, doi:10.1029/2010GL042430, 2010.

450 Bond-Lamberty, B., and Thomson, A.: Temperature-associated increases in the global soil
451 respiration record., *Nature*, 464, 579-582, doi:10.1038/nature08930, 2010.

452 Booth, B. B. B., Jones, C. D., Collins, M., Totterdell, I. J., Cox, P. M., Sitch, S., Huntingford,
453 C., Betts, R. A., Harris, G. R., and Lloyd, J.: High sensitivity of future global warming to land
454 carbon cycle processes, *Environ. Res. Lett.*, 7, 024002, doi:10.1088/1748-9326/7/2/024002,
455 2012.

456 Davidson, E. A., Belk, E., and Boone, R. D.: Soil water content and temperature as
457 independent or confounded factors controlling soil respiration in a temperate mixed hardwood
458 forest, *Global change biol.*, 4, 217-227, doi: 10.1046/j.1365-2486.1998.00128.x, 1998.

459 Foley, J. A., Levis, S., Prentice, I. C.: Coupling dynamic models of climate and vegetation,
460 *Global Change Biol.*, 4, 561–79, 1998.

461 Friedlingstein, P., Cox, P., Betts, R., Bopp, L., von Bloh, W., Brovkin, V., Cadule, P., Doney,
462 S., Eby, M., Fung, I., Bala, G., John, J., Jones, C., Joos, F., Kato, T., Kawamiya, M., Knorr, W.,
463 Lindsay, K., Matthews, H. D., Raddatz, T., Rayner, P., Reick, C., Roeckner, E., Schnitzler, K.
464 G., Schnur, R., Strassmann, K., Weaver, A. J., Yoshikawa, C., and Zeng, N.: Climate–carbon
465 cycle feedback analysis: Results from the C4MIP model intercomparison, *J. Clim.*, 19, 3337–
466 3353, doi:10.1175/JCLI3800.1, 2006.

467 Friedlingstein, P., Meinshausen, M., Arora, V. K., Jones, C. D., Anav, A., Liddicoat, S. K.,
468 and Knutti, R.: Uncertainties in CMIP5 climate projections due to carbon cycle feedbacks, *J.*
469 *Clim.*, 27, 511-525, doi:10.1175/JCLI-D-12-00579.1, 2014.

470 Gregory, J. M., Jones, C. D., Cadule P., and Friedlingstein P.: Quantifying Carbon Cycle
471 Feedbacks, *J. Clim.*, 22, 5232-5249, 2009.

472 Hashimoto, S., Carvalhais, N., Ito, A., Migliavacca, M., Nishina, K., and Reichstein, M.:



473 Global spatiotemporal distribution of soil respiration modeled using a global database,
474 Biogeosciences, 12, 4121-4132, doi:10.5194/bg-12-4121-2015, 2015.

475 Hoffman, F. M., Randerson, J. T., Arora, V. K., Bao, Q., Cadule, P., Ji, D., Jones, C. D.,
476 Kawamiya, M., Khatiwala, S., Lindsay, K., Obata, A., Shevliakova, E., Six, K. D., Tjiputra, J.
477 F., Volodin, E. M., and Wu, T.: Causes and implications of persistent atmospheric carbon
478 dioxide biases in Earth System Models, *J. Geophys. Res. Biogeosci.*, 119, 141-162, doi:
479 10.1002/2013JG002381, 2013.

480 Jung, M., Henkel, K., Herold, M., and Churkina, G.: Exploiting synergies of global land
481 cover products for carbon cycle modeling, *Remote. Sens. Environ.*, 101, 534–553, 2006.

482 Jung, M., Reichstein, M., and Bondeau, A.: Towards global empirical upscaling of
483 FLUXNET eddy covariance observations: validation of a model tree ensemble approach using
484 a biosphere model, *Biogeosciences*, 6, 2001–2013, doi:10.5194/bg-6-2001-2009, 2009.

485 Kirschbaum, M. U. F.: The temperature dependence of soil organic matter decomposition,
486 and the effect of global warming on soil organic C storage, *Soil Biol. Biochem.*, 27, 753–760,
487 1995.

488 Kutsch, W. L., Bahn, M., and Heinemeyer, A.: Soil carbon dynamics: An integrated
489 methodology, Cambridge: Cambridge University Press., 2009

490 Le Quer'e, C., Raupach, M. R., Canadell, J. G., Marland, G., Bopp, L., Ciais, P., Conway,
491 T. J., Doney, S. C., Feely, R. A., Foster, P., Friedlingstein, P., Gurney, K., Houghton, R. A.,
492 House, J. I., Huntingford, C., Levy, P. E., Lomas, M. R., Majkut, J., Metzl, N., Ometto, J. P.,
493 Peters, G. P., Prentice, I. C., Randerson, J. T., Running, S. W., Sarmiento, J. L., Schuster, U.,
494 Sitch, S., Takahashi, T., Viovy, N., van der Werf, G. R., and Woodward, F. I.: Trends in the
495 sources and sinks of carbon dioxide, *Nat. Geosci.*, 2, 831–836, doi:10.1038/ngeo689, 2009.

496 Liski, J., Ilvesniemi, H., Makel, A., Westman, K. J.: CO₂ emissions from soil in response to
497 climatic warming are overestimated – the decomposition of old soil organic matter is tolerant



- 498 of temperature, *Ambio*, 28, 171–174, 1999.
- 499 Lloyd, J. and Taylor, J. A.: On the Temperature Dependence of Soil Respiration, *Funct. Ecol.*,
- 500 8, 315–323, 1994.
- 501 Luo, Y., Wan, S., Hui, D., and Wallace, L. L.: Acclimatization of soil respiration to warming
- 502 in a tall grass prairie, *Nature*, 413, 622–625, doi:10.1038/35098065, 2001.
- 503 Luyssaert, S., Inglima, I., and Jung M.: The CO₂-balance of boreal, temperate and tropical
- 504 forest derived from a global database, *Global Change Biol*, 13, 2509–2537, 2007.
- 505 Malhi, Y., Baldocchi, D. D., and Jarvis, P. G.: The carbon balance of tropical, temperate and
- 506 boreal forests, *Plant, cell and environ.*, 22, 715–740, 1999.
- 507 Mao, J., Thornton, P. E., Shi, X., Zhao, M., and Post, W. M.: Remote Sensing Evaluation of
- 508 CLM4 GPP for the Period 2000–09, *J. Clim.*, 25, 5327–5342,
- 509 doi: <http://dx.doi.org/10.1175/JCLI-D-11-00401.1>, 2012.
- 510 Oleson, K., Lawrence, D. M., Bonan, G. B., Drewniak, B., Huang, M., Koven, C. D., Levis,
- 511 S., Li, F., Riley, W. J., Subin, Z. M., Swenson, S. C., Thornton, P. E., Bozbiyik, A., Fisher, R.,
- 512 Heald, C. L., Kluzek, E., Lamarque, J.-F., Lawrence, P. J., Leung, L. R., Lipscomb, W., Muszala,
- 513 S., Ricciuto, D. M., Sacks, W., Sun, Y., Tang, J., and Yang, Z.-L.: Technical Description of
- 514 version 4.5 of the Community Land Model (CLM), NCAR Technical Note NCAR/TN-
- 515 503+STR, Boulder, Colorado, 420 pp., 2013.
- 516 Qi, Y., Xu, M., and Wu, J.: Temperature sensitivity of soil respiration and its effects on
- 517 ecosystem carbon budget: nonlinearity begets surprises, *Ecolog. Model.*, 153, 131–142, 2002
- 518 Reichstein, M., Tenhunen, J. D., Rouspard, O., Ourcival, J. -M., Rambal, S., Dore, S., and
- 519 Valentini, R.: Ecosystem respiration in two Mediterranean evergreen Holm Oak forests:
- 520 drought effects and decomposition dynamics, *Funct. Ecol.*, 16, 27–39, doi: 10.1046/j.0269-
- 521 8463.2001.00597.x, 2002.
- 522 Running, S. W., Nemani, R. R., Heinsch, F. A., Zhao, M., Reeves, M., and Hashimoto, H.:



- 523 A Continuous Satellite-Derived Measure of Global Terrestrial Primary Production, *BioScience*,
524 54(6), 547-560, 2004.
- 525 Seller, P. J., Mintz, Y., Sud Y. C., and Dalcher, A.: A simple biosphere model (SiB) for use
526 within general circulation models, *J. Atmos. Sci.*, 43, 505–531, doi:10.1175/1520-
527 0469(1986)043<0505:ASBMFU>2.0.CO;2., 1986.
- 528 Sheffield, J., Goteti, G., and Wood, E. F.: Development of a 50-Year High-Resolution Global
529 Dataset of Meteorological Forcings for Land Surface Modeling, *J. Clim.*, 19, 3088-3111
530 doi: <http://dx.doi.org/10.1175/JCLI3790.1>, 2006.
- 531 Sitch, S., Smith, B., Prentice, I. C., Areneth, A., Bondeau, A., Cramer, W., Kaplan, J. O.,
532 Levis, S., Lucht, W., Sykes, M. T., Thonicke, K., and Venevsky, S.: Evaluation of ecosystem
533 dynamics, plant geography and terrestrial carbon cycling in the LPJ dynamic global vegetation
534 model, *Global Change Biol.*, 9, 161-185, 2003.
- 535 Suseela, V., Conant, R. T., Wallenstein, M. D., and Dukes, J. S.: Effects of soil moisture on
536 the temperature sensitivity of heterotrophic respiration vary seasonally in an old-field climate
537 change experiment, *Global Change Biol.*, 18, 336–348, 2012.
- 538 Tang, J., and Baldocchi, D. D.: Spatial–temporal variation in soil respiration in an oak–grass
539 savanna ecosystem in California and its partitioning into autotrophic and heterotrophic
540 components, *Biogeochem.*, 73, 183–207, 2005.
- 541 Taylor, B. R., Parkinson, D., and Parsons, W. F. J.: Nitrogen and Lignin Content as Predictors
542 of Litter Decay Rates: A Microcosm Test, *Ecology*, 70, 97-104.
543 Doi:<http://dx.doi.org/10.2307/1938416>, 1989.
- 544 Thornton, P. E., Doney, S. C., Lindsay, K., Moore, J. K., Mahowald, N., Randerson, J. T.,
545 Fung, I., Lamarque, J.-F., Feddema, J. J., and Lee, Y. -H.: Carbon-nitrogen interactions regulate
546 climate-carbon cycle feedbacks: results from an atmosphere-ocean general circulation model,
547 *Biogeosciences*, 6, 2099–2120, 2009.



548 Trumbore, S.: Carbon respired by terrestrial ecosystems – recent progress and challenges,
549 *Global Change Biol.*, 12, 141-153, DOI: 10.1111/j.1365-2486.2006.01067.x, 2006.

550 University of East Anglia Climatic Research Unit (CRU) [Jones Phil and Harris Ian]: CRU
551 TS3.21: Climatic Research Unit (CRU) Time-Series (TS) Version 3.21 of High Resolution
552 Gridded Data of Month-by-month Variation in Climate (Januray 1901–December 2012),
553 doi:10.5285/D0E1585D-3417-485F- 87AE-4FCECF10A992, 2013.

554 van't Hoff, J. H.: Lectures on Theoretical and Physical Chemistry. Part I. Chemical Dynamics,
555 Edward Arnold, London, 224-229, 1898.

556 Wan, S., and Luo Y.: Substrate regulation of soil respiration in a tallgrass prairie: Results of
557 a clipping and shading experiment, *Global Biogeochem. Cy.*, 17, 1054,
558 doi:10.1029/2002GB001971., 2003.

559 Wang, Y. P., Law, R. M., and Pak, B.: A global model of carbon, nitrogen and phosphorus
560 cycles for the terrestrial biosphere, *Biogeosciences*, 7, 2261–2282, doi:10.5194/bg-7-2261-
561 2010, 2010.

562 Xu, M., and Qi, Y.: Spatial and seasonal variations of Q10 determined by soil respiration
563 measures at a Sierra Nevadan forest, *Global Biogeochem. Cy.*, 15, 687 – 696, 2001.

564 Zhao, M. S., Heinsch, F. A., Nemani, R. R., and Running, S.W.: Improvements of the
565 MODIS terrestrial gross and net primary production global data set, *Remote Sens. Environ.*,
566 95, 164–176, doi:10.1016/j.rse.2004.12.011, 2005.

567 Zhou, T., Shi, P., Hui, D., and Luo, Y.: Global pattern of temperature sensitivity of soil
568 heterotrophic respiration (Q10) and its implications for carbon-climate feedback, *J. Geophys.*
569 *Res.*, 114, doi:10.1029/2008JG000850, 2009.

570

571

572



573

574 **Table 1.** Climatological averaged Q10 values by PFTs in CLM4

	Temperate	Boreal	Tropical	Shrub	B. Shrub	Grass	Crop
Averaged Q10 value	1.446	1.762	1.374	1.266	1.918	1.842	2.041

575

576

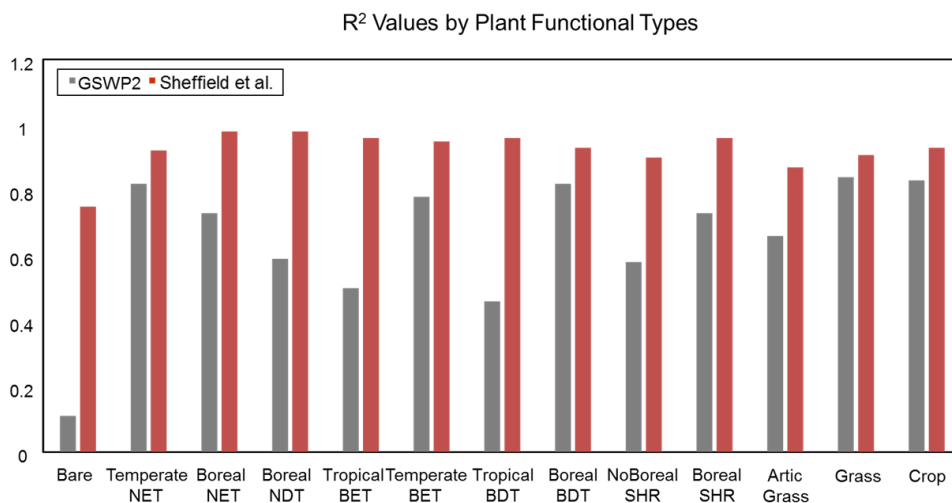
577

578



579

580



581

582 **Figure 1.** R-squared value in multiple regression by PFTs in CLM4 between soil respiration
583 data and soil temperature and moisture from GSWP2 multiple ensemble model data (grey bars)
584 and off-line model output forced by Sheffield data for 28 years (red bars).

585

586

587

588

589

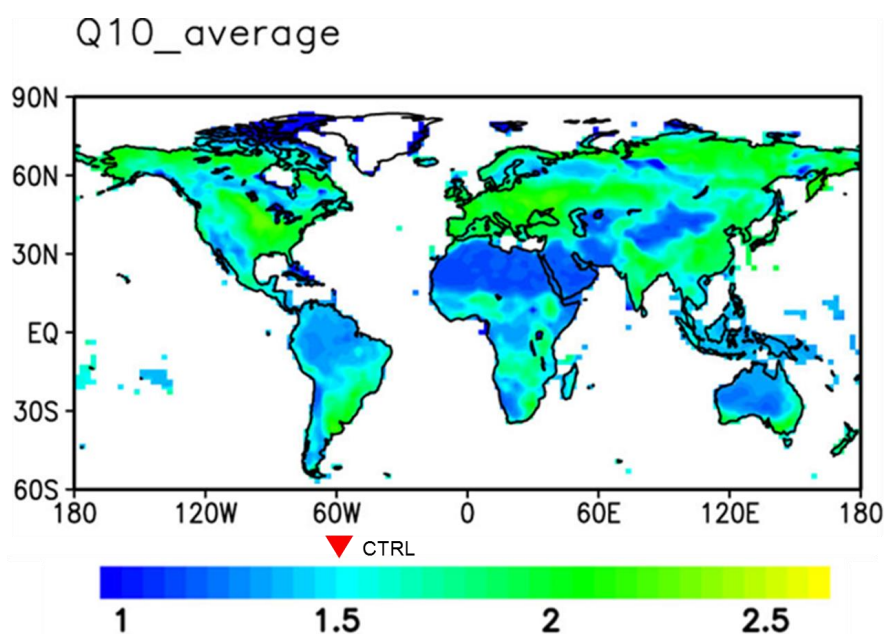
590

591

592



593



594

595 **Figure 2.** Climatological averaged Q10 spatial distribution in EXP experiment. Red filled
596 triangle indicates standard value of Q10 in CTL experiment.

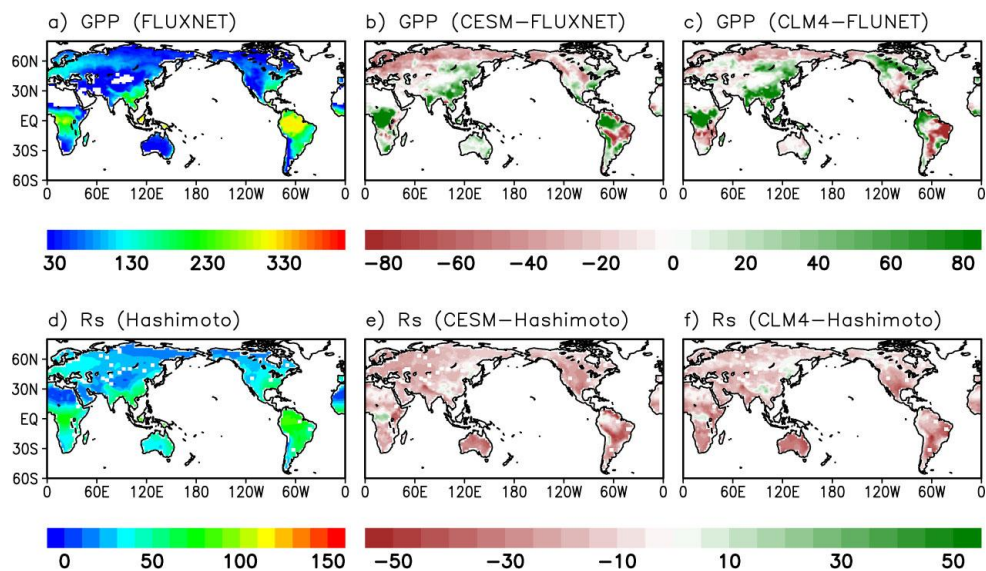
597

598

599

600

601



602

603 **Figure 3.** Spatial distribution of GPP(upper) and Rs (bottom) in the observation and bias

604 patterns of online full interactive simulation (CESM) and off-line (CLM4) experiment for 23

605 years (1983-2005). The unit is $\text{gC m}^2 \text{mon}^{-1}$.

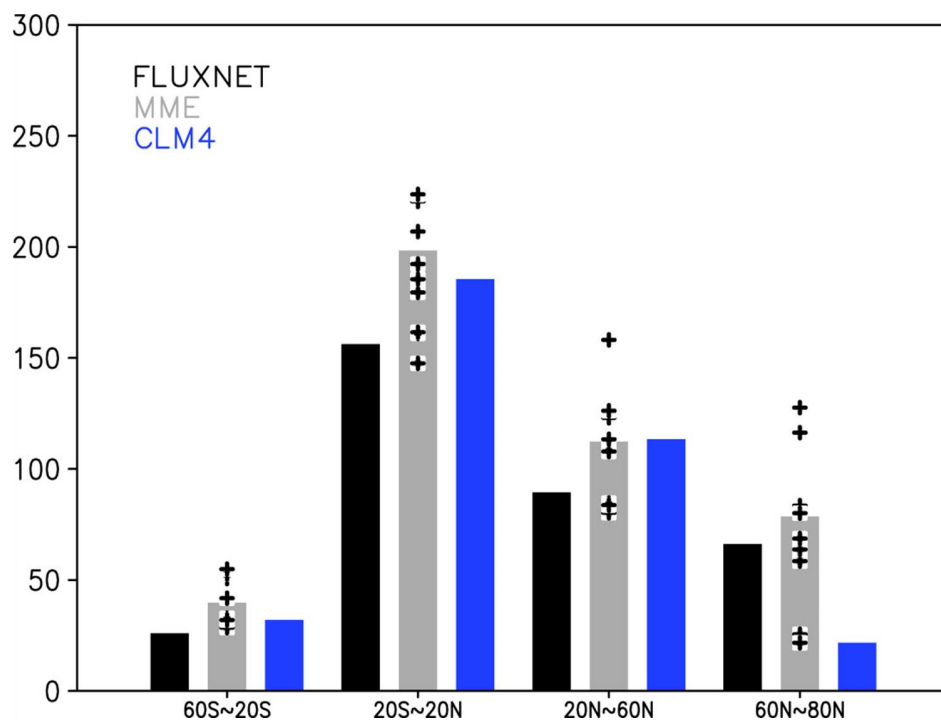
606

607

608

609

610



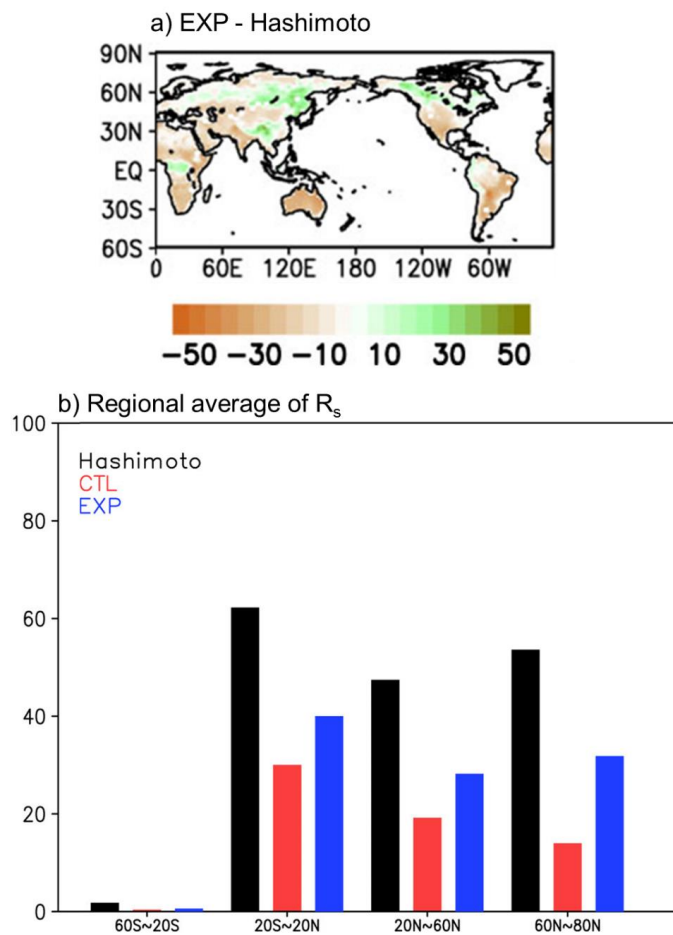
611

612 **Figure 4.** Regional averaged GPP in CMIP5 historical runs for 23 years (1983~2005). Black
613 bars indicate the FLUXNET. Grey bars are MME and symbol dots are individual models. Blue
614 bars show ESMs which are coupled with CLM4.

615



616

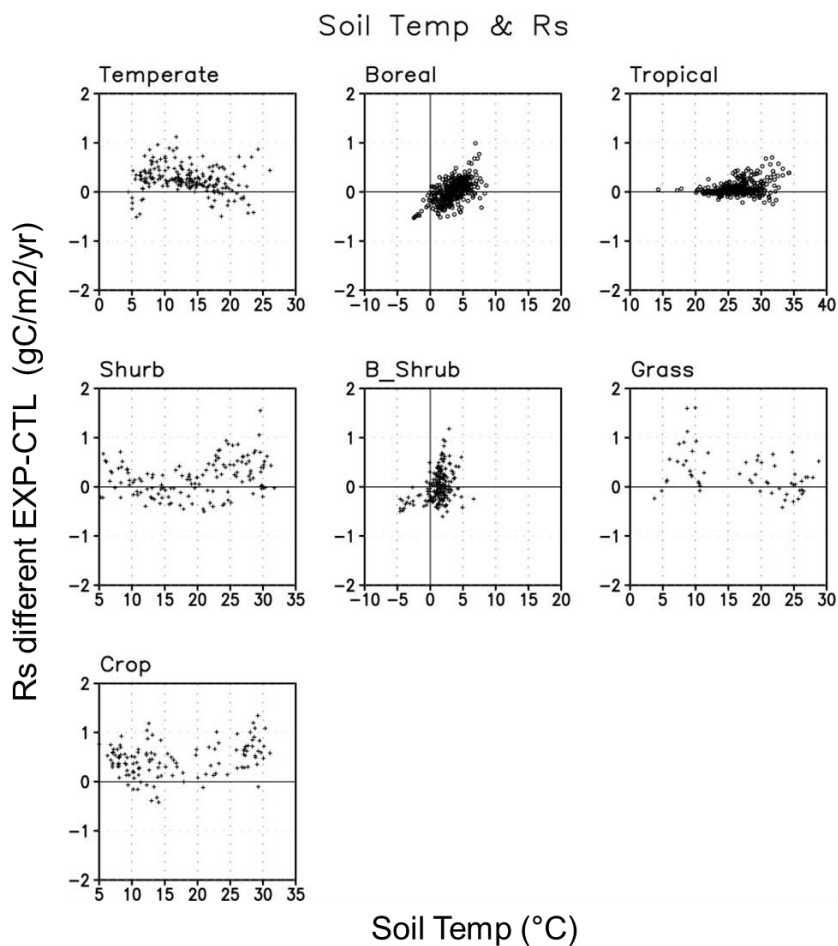


617

618 **Figure 5.** (a) shows the spatial distribution of bias pattern of R_s in EXP simulation. (b)
 619 indicates the comparison of the regional average of R_s between Hashimoto data (black bars),
 620 CTL simulation (red bars) and EXP experiment (blue bars).

621

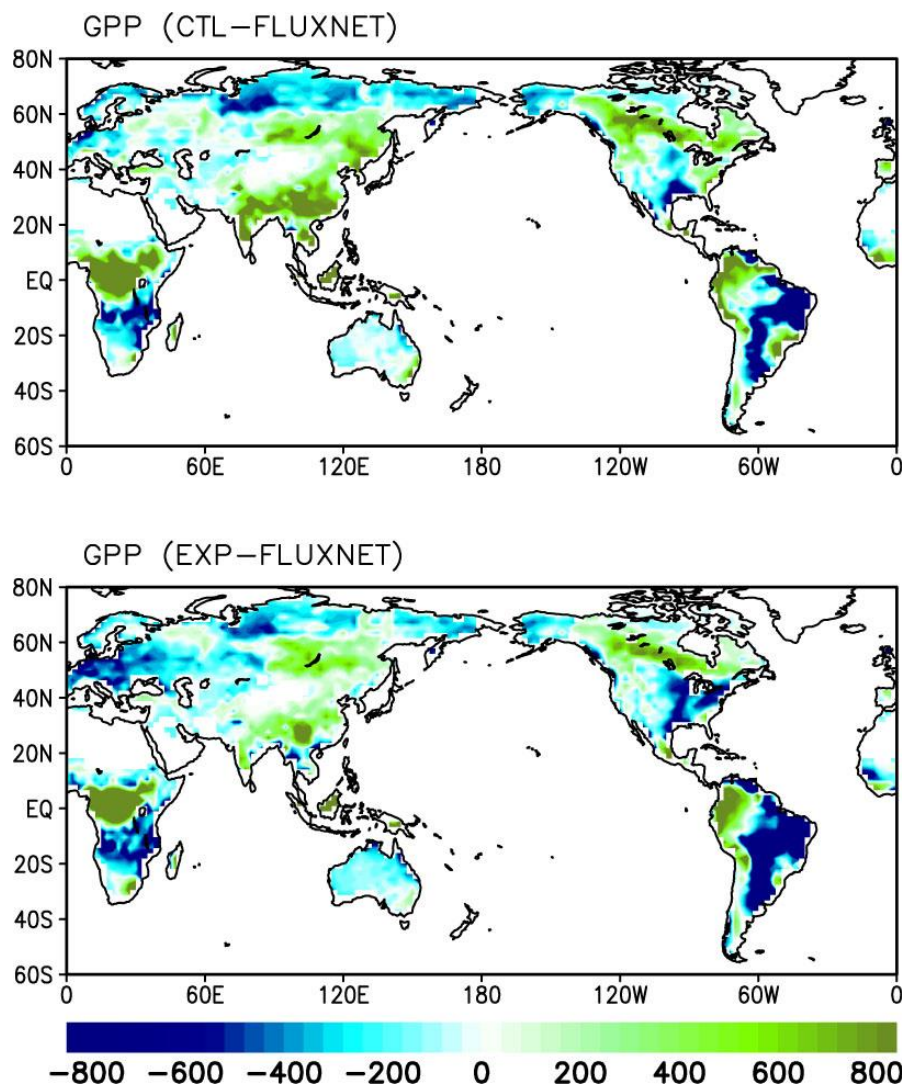
622



623

624 **Figure 6.** Scatter plots of change of Rs (y-axis) between EXP and CTL simulation as a
 625 function of soil temperature (x-axis). Each panel shows the plots for different PFTs that include
 626 temperate (temperate NET and BET), boreal (boreal NET, NDT, BDT), tropical (topical BET,
 627 BDT), Shrub, B_shrub (Boreal shrub), Grass(Grass) and Crop(Crop).

628



629

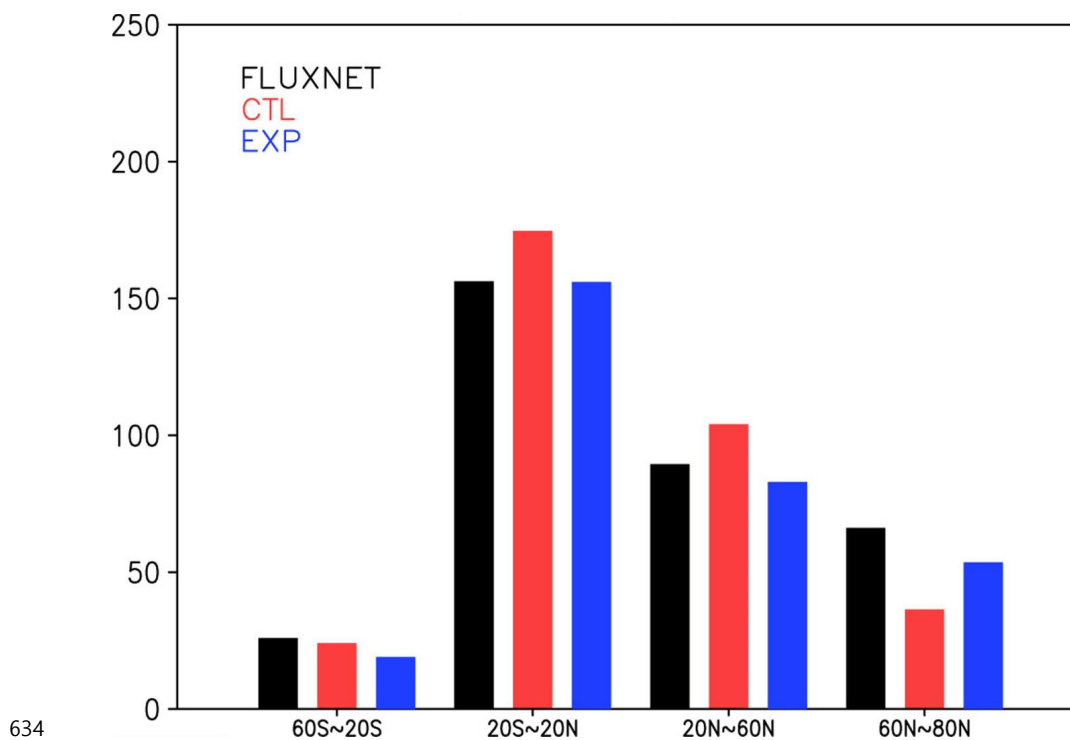
630

631

632

633

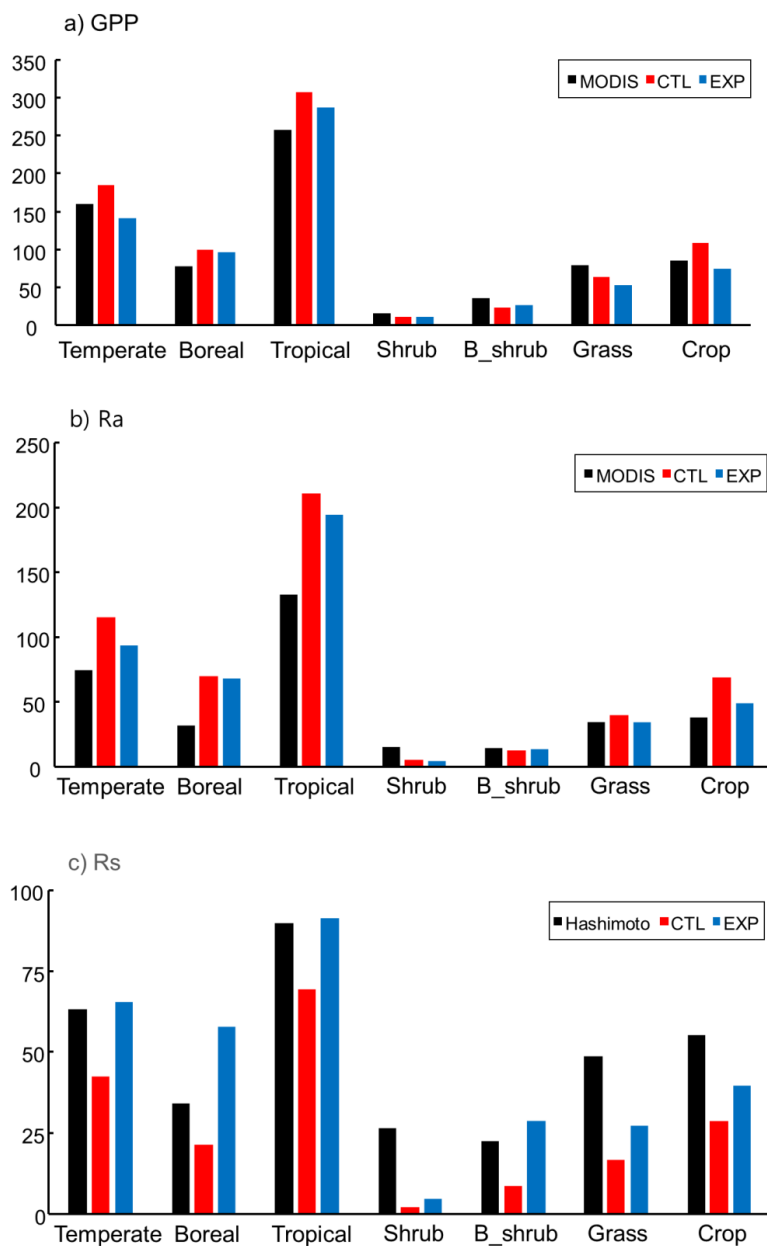
Figure 7. Bias of GPP spatial distribution in CTL and EXP comparing with FLUXNET during 23 years (1983-2005)



634

635 **Figure 8.** Regional averaged GPP in FLUXNET (black bars), CTL (red bars) and EXP (blue
636 bars).

637



638

639 **Figure 9.** Comparison of spatial average of GPP, Ra and Rs in observation (black bars),

640 CTL (red bars) and EXP (blue bars) by PFTs.